Characterization of $CuAlO_2$ Synthesized by ball milling assisted process in terms of Thermal, Structural, Morphological and Spectroscopic Analyses

Apurba Sarkar,[1] Soumya Mukherjee,[2#] Nandan Pakhira[1]

[1]*Department of Physics, Kazi Nazrul University, Asansol-713340, India*

[2]*Department of Metallurgical Engineering, Kazi Nazrul University, Asansol-713340, India*

Abstract: In the present work, delafossite $CuAlO_2$ nanoparticles are successfully synthesized via a solid-state high-energy ball milling approach, followed by controlled thermal treatment. The structural, thermal, vibrational/spectroscopic, and morphological characteristics of the synthesized material are investigated using thermogravimetric analysis (TGA), X-ray diffraction (XRD), Fourier Transform Infrared Spectroscopy (FTIR) and Scanning Electron Microscopy (SEM). TGA revealed the thermal stability and identified decomposition stages associated with precursor transformation and moisture desorption. XRD and FTIR analysis confirmed the formation of phase-pure $CuAlO_2$with rhombohedral crystal structure. SEM micrographs revealed agglomerated, irregularly shaped nanoparticles with rough surfaces and heterogeneous size distribution, while EDS confirmed the elemental homogeneity and absence of impurities. These findings establish the effectiveness of ball milling as a scalable route for synthesizing nanostructured $CuAlO_2$ with potential applications in optoelectronic and dielectric devices, where structural purity and microstructural features critically influence performance.

Keywords: $CuAlO_2$, Delafossite, Thermal analysis, Phase, Morphology, Bonding

1. Introduction

Thermoelectric materials have garnered significant research interest in recent few decades due to their ability to facilitate direct conversion between thermal and electrical energy, presenting promising avenues for sustainable power generation and waste heat recovery [1,2]. Among various classes of thermo-electric compounds, delafossite type oxides with the general formula ABO_2 have emerged as promising candidates owing to their structural tunability, chemical stability, and low toxicity. Notably, copper-based delafossites, including $CuFeO_2$, $CuCoO_2$, and $CuAlO_2$, have been actively explored for their potential in low-cost thermoelectric applications [3].

$CuAlO_2$ stands out among these compounds due to its abundant raw materials, simple synthesis routes and multifunctional physical properties. It has been extensively investigated not only as a thermoelectric material but also as a transparent conducting oxide (TCO), owing to its wide optical bandgap (>3.15 eV) and high visible-light transmittance (>80%) [4,5]. Furthermore, delafossite $CuAlO_2$ exhibits p-type semiconducting behaviour with a reported

bandgap in the range of 2.7-3.5 eV, depending on crystallinity and synthesis conditions [6-8]. Koumoto et al. have demonstrated its utility as a thermoelectric material, attributing its performance to its layered crystal structure and favourable electronic configuration [9].

Synthesis of nanocrystalline 3R-$CuAlO_2$ has been achieved through diverse methods, such as solid-state reaction with mechanical activation [10], hydrothermal metathesis [11], and sol–gel processing followed by calcination under controlled oxygen partial pressures [12,13]. These techniques influence the crystallographic phase, particle size, and defect chemistry, all of which critically affect the transport and optical properties. Notably, p-type dye-sensitized solar cells (DSSCs) utilizing $CuAlO_2$ nanoparticles as photocathode materials have demonstrated photocurrent densities ranging from 0.08 mA cm^{-2} to 0.98 mA cm^{-2}, highlighting the material's photovoltaic relevance [13,14].

In the present study, nanocrystalline $CuAlO_2$ is synthesized via high-energy ball milling, followed by thermal treatment to promote phase formation and structural refinement. A comprehensive characterization is carried out using X-ray diffraction (XRD), thermogravimetric analysis (TGA), Fourier-transform infrared spectroscopy (FTIR), and scanning electron microscopy coupled with energy-dispersive X-ray spectroscopy (SEM–EDS). The objective is to elucidate the structural evolution, thermal stability, and microstructural features of $CuAlO_2$ synthesized through a scalable and cost-effective approach, with an outlook toward potential applications in thermoelectric, transparent electronics, and photocatalytic systems.

2. Experimental section

2.1 Materials and Methods

At first high purity AR grade, CuO (99%) and Al_2O_3 (99%) powders were mixed and grounded very carefully for 10 h in an agate mortar at dry condition. A typical amount of CuO of 15.91 g and Al_2O_3 of 20.39 g were taken maintaining 1:1 molar ratio. Then the homogenized mixture was subjected to high-energy planetary ball milling using a Fritsch Pulverisette-5 mill. A ball-to-powder ratio of 5:1 was maintained with 5 mm tungsten carbide balls as grinding media in an acetone medium, operated at 370 rpm for a total duration of 100 hours. Following milling, the resultant powder was dried at 155 °C for 3 hours to remove residual organics. The dried powder was then calcined at 1200 °C in an alumina crucible under ambient air, employing a heating rate of 8 °C/min and a dwell time of 6 hours, followed by natural furnace cooling. The obtained $CuAlO_2$ powder was then divided into two portions. To facilitate the evaluation of density and porosity of the material one portion was compacted into disk shaped pellet of 8 mm diameter and 3 mm thickness under a uniaxial pressure of 10 MPa using a hydraulic press.

2.2 Characterizations

The thermal stability of the precursor was studied using thermogravimetric (TGA) thermal analysis techniques using Perkin-Elmer simultaneous TGA/DTA analyser, under N_2 atmosphere at heating rate 20 °C/min from 50 °C to 1200 °C.The structural characterization of the sample was done using a PAN Analytic X-ray diffractometer, employing Ni-filtered Cu

Kα radiation (λ = 1.5406 Å) at room temperature with a voltage of approximately 40 kV and a current of about 40 mA. The XRD patterns were collected from 10° to 70° with scanning steps 0.04° and time step of 0.1. Fourier transformed infrared (FTIR) spectra were recorded on a thermos scientific spectrometer (Nicolet 6700) with KBr pellets in transmittance mode, in the frequency range of 450cm^{-1}-4000 cm^{-1}. The surface morphology of the sample has been investigated using a scanning electron microscope (SEM) (Gemini SEM500, Zeiss, Oberkochen, Germany).

3. Results and discussion

3.1 Thermal analysis

Fig. 1 shows the TGA plot of the precursor under the flow of N_2 gas with the heating rate of 20 °C/min from 100 to 1200 °C. Avery small amount of weight loss occurs up to ~250 °C which could be due to the loss of adsorbed moisture and acetone by the precursor. The first weight loss peak located around 860 °C. This weight loss may be due to the formation of spinel phase $CuAl_2O_4$ from CuO and Al_2O_3 according to the reaction:

$$Al_2O_3 + CuO \rightarrow CuAl_2O_4 \quad (1)$$

The second peak around 1150 °C may be related to the decomposition of $CuAl_2O_4$ into delafossite $CuAlO_2$ phase,

$$CuAl_2O_4 \rightarrow CuAlO_2 + \frac{1}{2}O_2 \quad (2)$$

Based on the results of TGA, a temperature of 1200 °C is chosen to ensure the complete formation of $CuAlO_2$ form CuO and Al_2O_3.

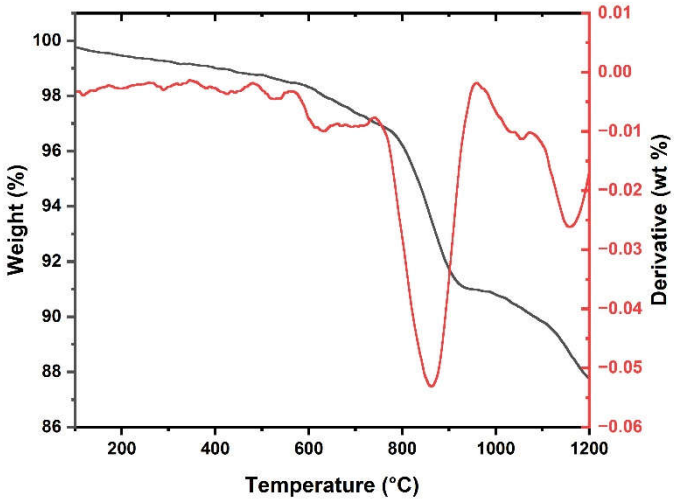

Fig. 1. Thermogravimetric analysis results of as-synthesized $CuAlO_2$ in N_2 atmosphere.

3.2 X-ray diffraction (XRD) analysis

The structural study is essential for optimizing the properties needed for various applications. The phase identification and lattice parameters are determined by an X-ray diffractometer. The X-ray diffraction pattern of the prepared samples sintered at 1200 °C for 6 h are shown in **Fig. 2.** As can be seen from the XRD patterns, it is observed that the position of the peaks

complies with the standard JCPDS card no. #04-007-5000. The prominent peaks observed at 2θ = ~ 31.35°, 36.37°, 37.57° corresponding to the planes (006), (101) and (012). The sharp peaks reveal that the samples are in good crystalline form. We found that the indexed peaks belonged to a rhombohedral unit cell of $CuAlO_2$with space group of R3m. We also observed minor one peak of $CuAl_2O_4$ (34.87°; #96-900-9678) and minor two peaks of unreacted Al_2O_3 (25.30°, 43.13°; #96-153-8459). The detected spinel $CuAl_2O_4$ peak may be arise during the cooling period due to its possible thermodynamical stability below 1000 °C as noted from TGA analysis.

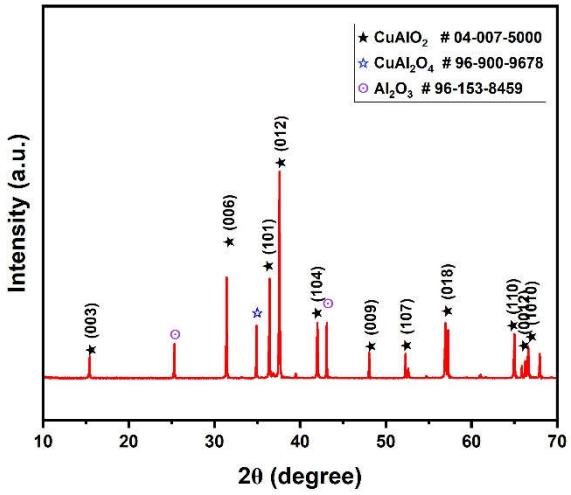

Fig. 2. X-ray diffraction pattern of as-synthesized CuAlO2 sample at 1200 °C.

The crystallite size (D) of $CuAlO_2$ has been calculated using Scherrer's formula:

$$D = \frac{K\lambda}{\beta \cos(\theta)} \quad (3)$$

Where, K is a constant equal to 0.9, β represents the full width at half maximum (FWHM) of the diffraction peak, θ is the diffraction angle, and λ = 1.5406 Å, is the wavelength of X-ray Cu Kα radiation source. From XRD, crystallite size and micro-strain using Williamson-Hall (W-H) method are calculated as follows:

$$\beta\cos\theta = (k\lambda/D) + \varepsilon\sin\theta \quad (4)$$

where ε is the micro-strain in the crystal. The W-H plot is shown in**Fig.3**.

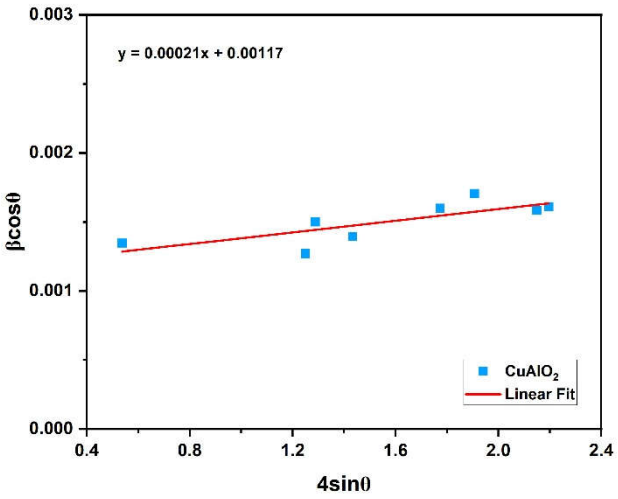

Fig. 3. Williamson-Hall plot of $CuAlO_2$ sample.

The lattice parameters of $CuAlO_2$ were calculated using the following equation:

$$\frac{1}{d^2} = \frac{h^2+k^2}{a^2} + \frac{l^2}{c^2}, \quad (5)$$

where d is the distance between crystalline planes and (hkl) are the Miller indices, and$a$ and c are lattice parameters and volume of unit cell was determined by using

$$V = \frac{\sqrt{3}}{2} a^2 c \quad (6)$$

Density plays an important role in controlling the properties of delafossite $CuAlO_2$. The theoretical density (ρ_{th})was calculated using the expression,

$$\rho_{th} = \frac{nM}{N_A V} \quad (7)$$

where, n is the number of atoms per unit cell, N_A is the Avogadro's number, M is the molecular weight and V is the volume of the unit cell of $CuAlO_2$, and the bulk density (ρ_B) was calculated using Archimede's principle as follow,

$$\rho_B = \frac{D}{W-S} \quad (8)$$

where, D is the dry weight, W is the saturated weight and S is the suspended weight.

The apparent porosity (P) is calculated using the relation,

$$P\,(\%) = \frac{W-D}{W-S} \times 100\,\% \quad (9)$$

The calculated lattice parameters, crystallite size, micro-strain, density, porosity for $CuAlO_2$ sample is summarized in **Table 1**.

Table 1. Calculated lattice parameters, crystallite size, micro-strain, density and porosity of as-synthesized $CuAlO_2$.

Sample	Lattice constants (Å)		Crystallite size (nm)		Micro-strain	Density (g/cm^{-3})		Relative density	Porosity (%)
	a=b	c	Scherrer	WH	(*10^{-3})	Bulk	Theoretical	(%)	
$CuAlO_2$	2.875	16.978	105	118	0.21	4.3	5.01	86%	14%

From the table it is observed that the bulk density (ρ_B) is lower than the theoretical density (ρ_{th}). This may be due to the existence of pores which are formed and developed during the sample preparation or the sintering process. The porosity of ceramic samples results from the two sources, intra-granular porosity, and intergranular porosity [15]. The intra-granular porosity depends mainly on the grain size. Thus, the total porosity can be written as,

$$P = P_{intra} + P_{inter} \quad (10)$$

3.2 FTIR analysis

The Fourier Transform Infrared (FTIR) spectra of the synthesized $CuAlO_2$ is shown in **Fig. 4**. It reveals critical insights into the functional groups and bonding environment, confirming phase formation and assessing the presence of residual species. A broad absorption band centred around 3450 cm^{-1}corresponds to O–H stretching vibrations [16], likely due to surface-adsorbed moisture or hydroxyl groups, a common feature in oxide-based nanomaterials exposed to ambient conditions. The accompanying band at 1640 cm^{-1} is attributed to H-O-H bending of molecular water [17]. Minor peaks observed in the 2850-2950 cm^{-1} range could be indicative of residual C-H stretching modes [18], potentially arising from organic precursors or trace milling contaminants. However, these are relatively weak, suggesting minimal surface-bound organic species, consistent with efficient processing. The most prominent fingerprint features occur in the 500-700 cm^{-1} region, which are associated with Cu-O stretching vibrations and lattice modes [19], characteristic of the delafossite $CuAlO_2$ structure. Additionally, a shoulder or band near 1000-1100 cm^{-1} may be ascribed to Al–O stretching in distorted AlO_6 geometries [20], supporting the successful incorporation of Al into the delafossite lattice.

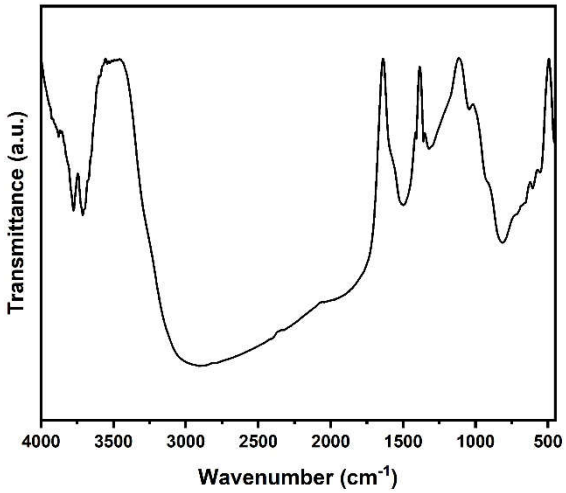

Fig. 4. FTIR spectra of as-synthesized $CuAlO_2$ sample.

3.3 SEM analysis

The microstructure of the synthesized $CuAlO_2$sample, as examined by Scanning Electron Microscopy (SEM), shown in **Fig. 5(a) and (b),** reveals vital information about particle morphology and surface characteristics. The SEM micrographs, captured at 5000x magnification corresponding to a 2 µm scale, display irregularly shaped and highly agglomerated particles, a feature commonly associated with the high-energy ball milling process. The agglomeration is likely driven by vander Waals interactions and high surface energy, particularly prevalent in nanoscale oxides. Particles exhibit non-uniform size distribution, spanning submicron to nanometric dimensions. In some portions polygonal features, flaky structures are noted. Individual particulates are roughly estimated to be about 0.5 µm to 0.1 µm. The surfaces are faceted and rough, indicative of polycrystalline growth and possible micro-strain within the lattice-features that may contribute to enhanced surface reactivity or defect-mediated optical behaviour. Roughness on surface of synthesized samples arises may be possibly due to porosity as noted from the experiment.

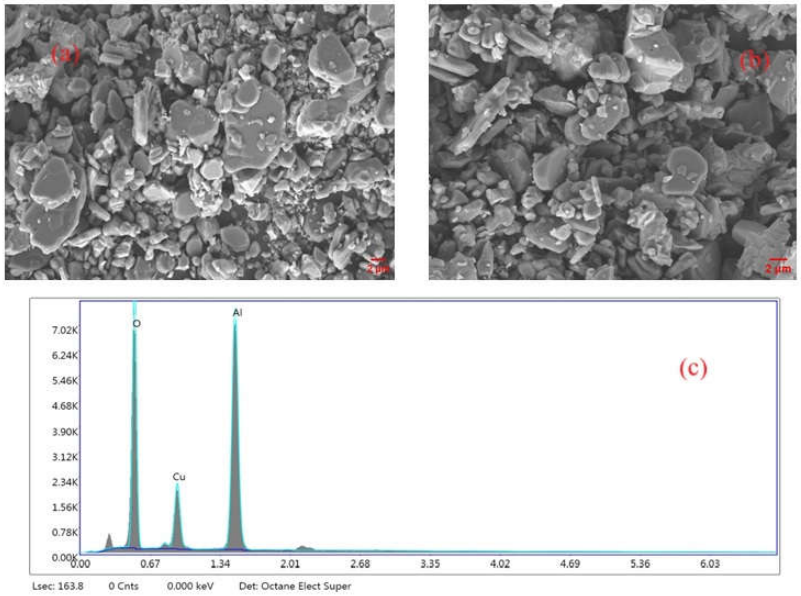

Fig. 5. (a), (b) SEM morphology of $CuAlO_2$ and (c) the elemental analysis by EDS.

Complementary Energy Dispersive X-ray Spectroscopy (EDS) as shown in **Fig. 5. (c)** confirms the elemental composition of the sample. The spectrum reveals distinct peaks corresponding to copper (Cu), aluminium (Al), and oxygen (O), with no evidence of extraneous elements, thus validating the compositional purity of the delafossite $CuAlO_2$ phase. The stoichiometric presence of Cu and Al suggests successful precursor incorporation during synthesis and thermal processing. The observed morphology and clean elemental signature render the synthesized $CuAlO_2$ promising for optoelectronic and dielectric applications, where purity and microstructural features play a pivotal role. The elemental composition details of the $CuAlO_2$ sample are given in **Table 2**.

Table 2. The elemental composition details of the $CuAlO_2$ sample.

Element	Weight (%)	Atomic (%)
O (K series)	35.17	51.95
Cu (L series)	17.34	6.45
Al (K series)	47.49	41.60

4. Conclusions

In summary, phase-pure $CuAlO_2$samples are successfully synthesized through a high-energy ball milling-assisted solid-state route followed by thermal treatment. The structural, thermal, vibrational, and microstructural characteristics are comprehensively evaluated using XRD, TGA, FTIR, and SEM-EDS techniques. XRD analysis confirmed the formation of nanocrystalline $CuAlO_2$ with a rhombohedral (R3m space group) delafossite structure, while TGA demonstrated the thermal stability and purity of the material with negligible weight loss beyond 800 °C. FTIR spectra revealed distinct Cu–O and Al–O lattice vibrational modes, along with minor O–H and C–H features attributed to surface-adsorbed species. SEM analysis highlighted agglomerated nanoparticles with irregular morphologies, and EDS confirmed the elemental homogeneity without detectable impurities. The combined results affirm the effectiveness of high-energy ball milling as a viable synthesis route for fabricating delafossite $CuAlO_2$ with high phase purity at about sub-micron to nanoscale features for advanced applications in optoelectronic, dielectric, and energy-related technologies.

Conflicts of interest

The authors declare no competing interests.

Acknowledgements

We would like to thank Materials Science Centre, IIT Kharagpur, and Jadavpur University for providing the facility of synthesis and characterizations. One of us (AS) wishes to thank the CSIR-UGC, Govt. of India, for awarding him a Senior Research Fellowship (SRF) during the execution of this work.

References

[1] Bell, Lon E. "Cooling, heating, generating power, and recovering waste heat with thermoelectric systems." *Science* 321, no. 5895 (2008): 1457-1461. https://doi.org/10.1126/science.1158899.

[2] Liu, Liping. "A continuum theory of thermoelectric bodies and effective properties of thermoelectric composites." *International Journal of Engineering Science* 55 (2012): 35-53. https://doi.org/10.1016/j.ijengsci.2012.02.003.

[3] Nagarajan, R., N. Duan, M. K. Jayaraj, J. Li, K. A. Vanaja, A. Yokochi, A. Draeseke, Janet Tate, and A. W. Sleight. "p-Type conductivity in the delafossite structure." *International Journal of Inorganic Materials* 3, no. 3 (2001): 265-270. https://doi.org/10.1016/S1466-6049(01)00006-X.

[4]Tawada, Y., Hy Okamoto, and Y. Hamakawa. "a-SiC: H/a-Si: H heterojunction solar cell having more than 7.1% conversion efficiency." *Applied PhysicsLetters* 39, no. 3, (1981): 237-239. https://doi.org/10.1063/1.92692.

[5] Kawazoe, Hiroshi, Hiroshi Yanagi, Kazushige Ueda, and Hideo Hosono. "Transparent p-type conducting oxides: design and fabrication of pn heterojunctions." *MRS Bulletin* 25, no. 8 (2000): 28-36. https://doi.org/10.1557/mrs2000.148.

[6] Zhang, Yongjian, Zhengtang Liu, Duyang Zang, and Liping Feng. "Structural and opto-electrical properties of Cu–Al–O thin films prepared by magnetron sputtering method." *Vacuum* 99 (2014): 160-165.https://doi.org/10.1016/j.vacuum.2013.05.019.

[7] Ahmed, Jahangeer, Colin K. Blakely, Jai Prakash, Shaun R. Bruno, Mingzhe Yu, Yiying Wu, and Viktor V. Poltavets. "Scalable synthesis of delafossite CuAlO2 nanoparticles for p-type dye-sensitized solar cells applications." *Journal of alloys and compounds* 591 (2014): 275-279.https://doi.org/10.1016/j.jallcom.2013.12.199.

[8] Yu, Ruei-Sung, and Hui-Hsun Yin. "Structural and optoelectronic properties of p-type semiconductor CuAlO2 thin films." *Thin Solid Films* 526 (2012): 103-108.https://doi.org/10.1016/j.tsf.2012.11.033.

[9] Koumoto, Kunihito, Hisashi Koduka, and Won-Seon Seo. "MaterialsCommunicationJOURNAL OF." *J. Mater. Chem* 11 (2001): 251-252. https://doi.org/10.1039/B006850K.

[10] Miclau, M., N. Miclau, R. Banica, and D. Ursu. "Effect of polymorphism on photovoltaic performance of CuAlO2 delafossite nanomaterials for p-type dye-sensitized solar cells application." *Materials Today: Proceedings* 4, no. 7 (2017): 6975-6981.https://doi.org/10.1016/j.matpr.2017.07.027.

[11]Gao, Shanmin, Yan Zhao, Pingping Gou, Nan Chen, and Yi Xie. "Preparation of CuAlO2nanocrystalline transparent thin films with high conductivity." *Nanotechnology* 14, no. 5 (2003): 538.https://doi.org/10.1088/0957-4484/14/5/310.

[12]Ghosh, C. K., S. R. Popuri, T. U. Mahesh, and K. K. Chattopadhyay. "Preparation of nanocrystalline CuAlO 2 through sol–gel route." *Journal of sol-gel science and technology* 52 (2009): 75-81.https://doi.org/10.1007/s10971-009-1999-x.

[13]Ahmed, Jahangeer, Colin K. Blakely, Jai Prakash, Shaun R. Bruno, Mingzhe Yu, Yiying Wu, and Viktor V. Poltavets. "Scalable synthesis of delafossite CuAlO2 nanoparticles for p-type dye-sensitized solar cells applications." *Journal of alloys and compounds* 591 (2014): 275-279.https://doi.org/10.1016/j.jallcom.2013.12.199.

[14]Miclau, M., N. Miclau, R. Banica, and D. Ursu. "Effect of polymorphism on photovoltaic performance of CuAlO2 delafossite nanomaterials for p-type dye-sensitized solar cells application." *Materials Today: Proceedings* 4, no. 7 (2017): 6975-6981.https://doi.org/10.1016/j.matpr.2017.07.027.

[15] Casini, Francesca, Giulia MB Viggiani, and Sarah M. Springman. "Breakage of an artificial crushable material under loading." *Granular matter* 15 (2013): 661-673. https://doi.org/10.1007/s10035-013-0432-x.

[16] BOYRAZ, CİHAT, ADİL GÜLER, Ö. Karataş, P. Aksu, M. Alphan, and L. Arda. "The investigation of effect of defects on the structural, optical, and magnetic properties of CuAlO2." *Acta Physica Polonica A* 142, no. 4 (2022). https://doi.org/10.12693/aphyspola.142.464.

[17] Ghosh, C. K., S. R. Popuri, T. U. Mahesh, and K. K. Chattopadhyay. "Preparation of nanocrystalline CuAlO2 through sol–gel route." *Journal of sol-gel science and technology* 52 (2009): 75-81.https://doi.org/10.1007/s10971-009-1999-x.

[18] Banerjee, A. N., and K. K. Chattopadhyay. "Size-dependent optical properties of sputter-deposited nanocrystalline p-type transparent CuAlO2 thin films." *Journal of Applied Physics* 97, no. 8 (2005).https://doi.org/10.1063/1.1866485.

[19] Kim, Jong Kuk, Sang Su Kim, and Won-Jeong Kim. "Sol–gel synthesis and properties of multiferroic BiFeO3." *Materials Letters* 59, no. 29-30 (2005): 4006-4009.https://doi.org/10.1016/j.matlet.2005.07.050.

[20] Hou, Lei, Yu-Dong Hou, Man-Kang Zhu, Jianlan Tang, Jing-Bing Liu, Hao Wang, and Hui Yan. "Formation and transformation of ZnTiO3 prepared by sol–gel process." *Materials Letters* 59, no. 2-3 (2005): 197-200.https://doi.org/10.1016/j.matlet.2004.07.046.